Measurement 183 (2021) 109888

Contents lists available at ScienceDirect

Measurement

journal homepage: www.elsevier.com/locate/measurement

# Detection and manipulation of the transverse motion of neutral molecules in a Stark decelerator

Piotr Wcisło [a,b,*], Hao Wu [a,c], David Reens [a,d], Alexander Aeppli [a], Jun Ye [a]

[a] JILA, National Institute of Standards and Technology and the University of Colorado, Department of Physics, University of Colorado, Boulder, CO 80309-0440, USA
[b] Institute of Physics, Faculty of Physics, Astronomy and Informatics, Nicolaus Copernicus University in Toruń, Grudziadzka 5, 87-100 Torun, Poland
[c] Department of Physics and Astronomy, University of California, Los Angeles, CA 90095, USA
[d] Lincoln Laboratory, Massachusetts Institute of Technology, Lexington, MA 02420, USA

ARTICLE INFO

*Keywords:*
Measurement of cold molecules dynamics
Stark deceleration
Delta kick cooling

ABSTRACT

By enabling precise control over longitudinal velocity of neutral molecules, Stark deceleration has become an important tool for studying cold molecular collisions. However, the information about transverse motion is often hard to extract and to some extent beyond control. Here we demonstrate a new experimental approach that allows us to observe the transverse phase-space distribution of molecules within a Stark decelerator. The transverse dynamics can be tracked along the decelerator, which can be used to measure the initial transverse phase-space distribution of the molecules. The observed frequency of the transverse oscillations agrees well with the one determined from electric field distribution. Thermalization of the molecules at the decelerator entrance must be accounted for in our Monte Carlo simulations of the molecules dynamics to reach agreement with experimental data. We introduce two approaches of manipulating transverse modes. In the first method, a free-flight pulse is introduced to achieve a short phase-space stretching, an equivalent technique to delta kick cooling [Phys. Rev. Lett. 78, 2088 (1997)]. In the second mode we enforce phase-space rotation by varying the applied voltage. Both modes allow us to manipulate the transverse phase-space distribution and, in particular, allow us to tune (in a well-controlled way) the anisotropy of the phase-space distribution.

## 1. Introduction

The idea of using inhomogeneous electric fields to manipulate beams of neutral molecules was proposed almost a hundred years ago [1]. For a long time it was used only for deflecting molecular beams [2]. Two decades ago, the first successful deceleration of neutral molecules was demonstrated [3] for the metastable CO molecule. Since then, Stark deceleration has been implemented for many other molecular species [4–7] and used to load molecules into electrostatic [8], magnetic [9], and hybrid [10,11] traps, study high-resolution low-energy collisions [12,13] and even search for variability in fundamental constants [14]. Recently, Stark decelerators were implemented in the fountain [15] and synchrotron [16] configurations.

The previous works devoted to the operation of the Stark decelerator were mostly focused on the phase-space dynamics in the longitudinal direction, see for instance Refs. [5,17,18]. In Refs. [19–22], coupling between longitudinal and transverse degrees of freedom was discussed and its influence on the deceleration efficiency. Recently, new schemes for switching the electric field were developed [23], considerably improving the transverse confinement and, hence, the deceleration efficiency.

In this paper, we demonstrate an experimental technique that allows us to observe and manipulate the transverse phase-space distribution in a Stark decelerator. Our technique is to study perturbations of the simplest voltage configuration that can be applied to a decelerator, referred to here as DC guiding. In this mode the electric field is static and the molecules experience an effective trapping potential in the transverse dimensions. In principle, it should be possible to extend this approach to measure and manipulate the transverse phase-space distribution in bunching or slowing modes (at this point it is difficult to predict whether the degree of control would be better or worse in other modes). We perturb the DC guiding mode by briefly turning off the guide voltage at a specific time during the transit. By varying the turn-off time, transverse dynamics can be tracked along the entire propagation path within the decelerator, see Section 3. We use Monte Carlo simulations to interpret the measured oscillation signal in terms of

* Corresponding author at: Institute of Physics, Faculty of Physics, Astronomy and Informatics, Nicolaus Copernicus University in Toruń, Grudziadzka 5, 87-100 Torun, Poland.
*E-mail address:* piotr.wcislo@umk.pl (P. Wcisło).

https://doi.org/10.1016/j.measurement.2021.109888
Received 8 April 2021; Received in revised form 18 June 2021; Accepted 11 July 2021
Available online 17 July 2021
0263-2241/© 2021 The Authors. Published by Elsevier Ltd. This is an open access article under the CC BY-NC-ND license (http://creativecommons.org/licenses/by-nc-nd/4.0/).

evolution of the transverse phase-space distribution. A good agreement is reached between simulations and measured signal after including a simple model of molecule thermalization at the decelerator entrance. In addition, we use the strategy of the off-window to manipulate the transverse phase-space distribution and, in particular, to increase and decrease (in a well controlled way) the anisotropy of the phase-space distribution, see Section 4. A part of the manipulation sequence tested in this work is equivalent to the delta kick cooling (DKC) [24] in the transverse directions.

## 2. Experimental setup

Fig. 1(a) shows a simplified scheme of our experimental setup. The hydroxyl radicals (OH) are generated from water molecules by electric discharge and then cooled to sub-Kelvin temperatures during the supersonic expansion process [25]. We use an Even-Lavie valve [26] to generate short pulses of OH molecules seeded in a neon buffer gas. To reduce the clogging effect [25] at the entrance of the decelerator, we place a 3-mm diameter skimmer between the valve and decelerator. The low-field-seeking OH molecules ($^2\Pi_{3/2}$, $v = 0$, $J = 3/2$, $f$-parity, $m_J = 3/2$) travel through the decelerator with a longitudinal ($z$ direction) speed of 813 m/s. After approximately 2 ms, the molecules exit the decelerator and enter the detection stage, where they are illuminated with a 282 nm pulsed dye laser and the 313 nm fluorescence signal is collected with a photomultiplier tube. The fluorescence signal is proportional to the population. The detection volume covers nearly all the molecules leaving the decelerator. The system runs at a 10 Hz repetition rate.

The decelerator consists of 333 pairs of high-voltage pins separated by 2 mm and spaced 5 mm apart along the length of the decelerator [23,27,28]. Since alternate pairs have orthogonal orientations, the effective confinement in the transverse ($x$-$y$) direction can be treated as a 2-dimensional trap (2 mm × 2 mm square). Since in the DC guiding mode neither confinement nor deceleration are present in the longitudinal direction (a constant voltage, $\Delta V$, is kept across the nearby pin pairs, see Fig. 1D in Ref. [23]), the longitudinal temperature of OH ensemble is 250 mK and almost constant during propagation through the decelerator. Thanks to the absence of any longitudinal dynamics, transverse dynamics take center stage. Due to the effective trapping potential in the transverse direction, and due to an incomplete phase space filling in this potential, the molecules undergo periodic transverse motion, which macroscopically is manifested as oscillations of transverse temperature In this work the system is not in thermal equilibrium; by temperature we mean average kinetic energy expressed in units of Kelvin, which is determined as: $m\langle v_x^2 + v_y^2\rangle/(2k_B)$, where $m$ is the molecule mass, $k_B$ the Boltzmann constant and $\langle \dots \rangle$ the average over the considered ensemble. Figs. 1(b) and (c) illustrate Monte Carlo simulations of the transverse temperature as a function of time and the corresponding evolution of the phase-space density (PSD) in one of the transverse directions.

For most of the cases considered in this paper, it is sufficient to base our simulations on a harmonic approximation of the effective transverse potential. We have also performed full simulations of molecular dynamics in an actual potential, such as the predicted values of the trap frequency shown in Fig. 2. Doing so allows us to confirm that the effective harmonic trap approximation works well for the first oscillation cycle (which is relevant for our quantitative analysis from Section 3) and to link the frequency of transverse oscillations with the geometry of the decelerator and the applied voltage. The harmonic approximation neglects the spiral-like character of the PSD rotation due to potential anharmonicity and couplings between the transverse and longitudinal motions, which would effectively manifest as a damping of the oscillations of the OH signal. It is seen in the top panel in Fig. 2 that the behavior of the signal is far different from simple damped oscillations, hence it is not the harmonic approximation which limits the capability to model the experimental signals. The $\tilde{x}$ and $\tilde{v}_x$ variables

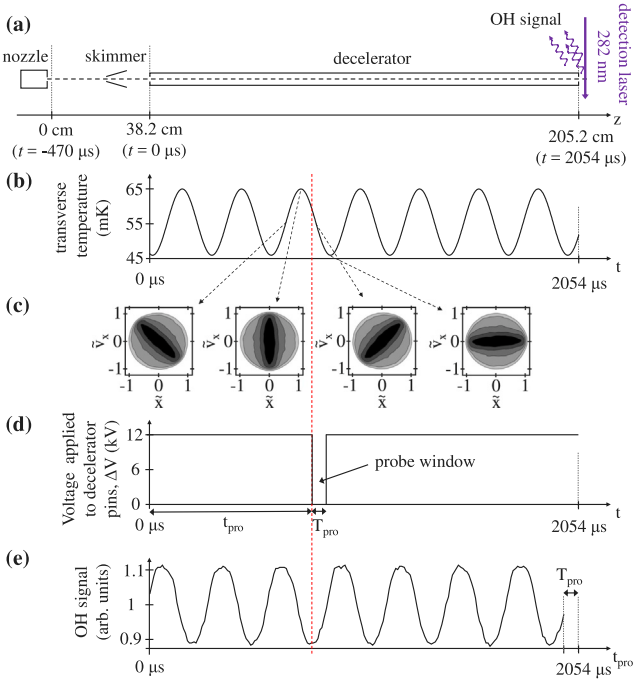


**Fig. 1.** Simulated transverse oscillations in a Stark decelerator. (a) Experimental setup. (b) Simulations of the transverse temperature of OH molecules. (c) Simulations of evolution of the phase-space distribution, corresponding to the four time steps shown in (b). (d) Voltage applied across nearby pin pairs of the decelerator. The DC voltage is interrupted for duration $T_{\mathrm{pro}}$. The losses depend on the probe window delay time ($t_{\mathrm{pro}}$) from the start of the decelerator. (e) Simulations of the OH signal after the decelerator as a function of $t_{\mathrm{pro}}$. Note that, in contrast to panels (b) and (d), the horizontal axis in panel (e) is not the actual time but a position of the probe window ($t_{\mathrm{pro}}$). The red dashed vertical line indicates the phase relation between panels (b), (d) and (e).

from Fig. 1(c) are the normalized x-components of the position and velocity defined as $\tilde{x} = x/x_0$ and $\tilde{v}_x = v_x/v_0$, where $x_0$ (= 1 mm) is one half the pin spacing in transverse direction and $v_0 = \omega x_0$, where $\omega$ is the angular frequency of the trap in the transverse direction. For instance, while $\Delta V = 12$ kV is applied across the pin pair, the angular frequency is $\omega = 2\pi \times 1.76$ kHz. Note that the temperature oscillations, shown in Fig. 1, reflect the breathing oscillation mode of the trapped molecules, hence its frequency, $f$, is two times larger, i.e., $2 \times 1.76$ kHz = 3.52 kHz.

## 3. Detection of the transverse motion

In this section, we demonstrate a technique that provides experimental observation of the evolution of the transverse phase-space distribution. Although the laser detection occurs after the molecules exit the decelerator, this technique lends insight into the molecules transverse dynamics along the entire propagation path within the decelerator. We achieve this by introducing a probe window (whose duration is $T_{\mathrm{pro}}$), see Fig. 1(d). We turn off the voltage applied to the decelerator for a period of $T_{\mathrm{pro}}$, at a tunable delay. Usually we choose $T_{\mathrm{pro}}$ to be close to a quarter of the breathing-mode oscillation period, which for $\Delta V = 12$ kV is 284 µs, hence $T_{\mathrm{pro}} = 71$ µs. The voltage switching time in our setup is smaller than 1 µs. Depending on the delay of the probe window, $t_{\mathrm{pro}}$, with respect to the initial phase of the transverse oscillations, the ensemble of molecules experience different losses. When the transverse temperature reaches its minimum value, the molecules on average have slower transverse speeds compared to transverse temperature maxima and, hence, are less probable to escape the trap region during the probe window. In Fig. 1(e), we show the simulations of the laser induced fluorescence signal as a function of $t_{\mathrm{pro}}$. The red dashed vertical line indicates the phase relation between

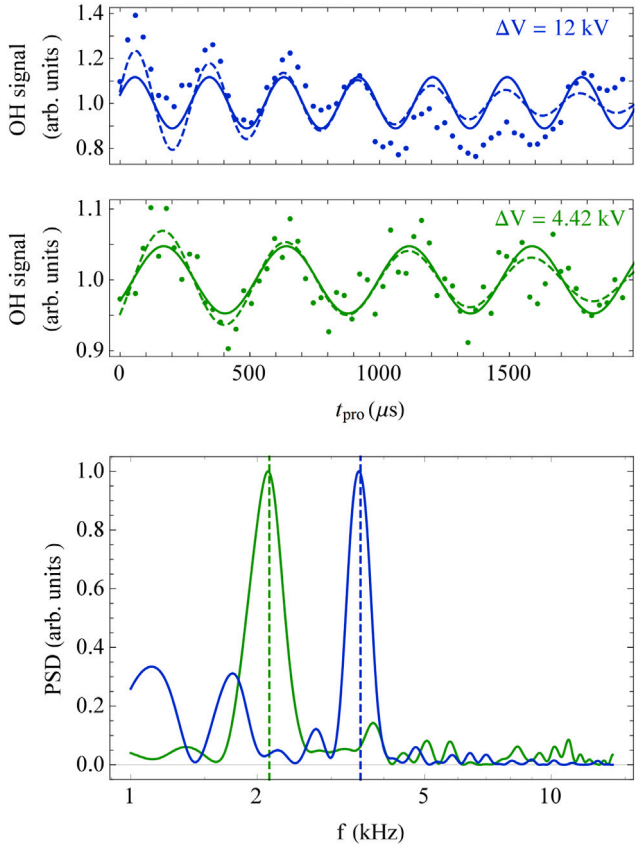


**Fig. 2.** Measurement of the breathing mode of transverse oscillations. The middle and top panels show the OH signal measured after the decelerator as a function of the probe window delay ($t_{pro}$), for $\Delta V$ = 4.42 and 12 kV, respectively. In all the panels, the green and blue color curves correspond to 4.41 and 12 kV, respectively. Points are experimental data. The solid lines are sine fits and dashed lines are damped sine fits. The bottom panel shows the spectra of the oscillations from the top and middle panels. The vertical dashed lines in the bottom panel indicates the simulated frequencies (2.14 and 3.52 kHz for $\Delta V$ = 4.42 and 12 kV). (For interpretation of the references to color in this figure legend, the reader is referred to the web version of this article.)

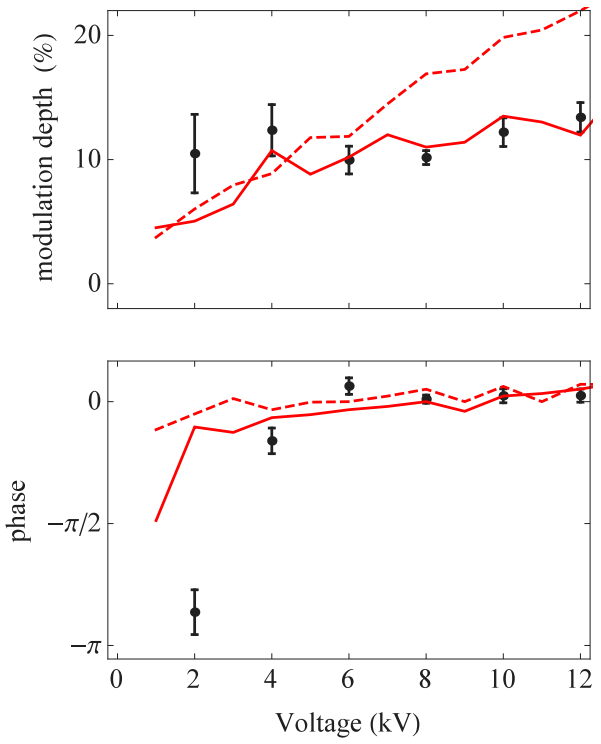


**Fig. 3.** Modulation depth (i.e., the ratio of oscillation amplitude to DC component of the signal) and phase of the breathing mode of transverse-motion oscillations as a function of voltage applied to decelerator pins. The amplitude is normalized to the offset (the mean value) in the OH signal. The black points are experimental data and the red lines are results of our simulations. The dashed and solid lines are the results of simulations without and with molecules thermalization, respectively. Both the experiment and simulations are carried out for the probe window duration $T_{pro} = 0.25 \times T_{breath}$, where $T_{breath}$ is the voltage-dependent breathing-mode period. The error bars are $1\sigma$ standard uncertainties retrieved from the fits.

panels (b), (d) and (e). The largest losses, corresponding to a minimum in Fig. 1(e), occur when the probe window starts approximately a quarter oscillation period after the maximum of transverse temperature when the molecules still have close-to-maximum speeds, but already managed to migrate out of the center of the transverse trap. Similarly, the smallest losses, and maximal OH signal in Fig. 1(e), occur when the probe window starts approximately a quarter oscillation period after the minimum of transverse temperature when the molecules on average have small speeds and start traveling towards the trap center. The exact value of the phase shift between the laser induced fluorescence signal and transverse temperature oscillations depends on the conditions of the experiment (for instance, $T_{pro}$). Figs. 1(b), (c) and (e) are generated with the same Monte Carlo simulations parameters. The curve from panel (e) is noisier due to much larger numerical cost required.

In the top and middle panels in Fig. 2, we show the actual measurements of the breathing mode of transverse oscillations, which are exactly the same quantity as the simulation shown in Fig. 1(e). The blue and green colors correspond to $\Delta V$ = 12 and 4.42 kV, respectively. The points are experimental data and solid lines are sinusoidal fitting, $\propto \sin(\omega t_{pro} + \phi)$, of which $\phi$ is initial phase of oscillation and determined by the duration of free-flight between the valve and the entrance of the Stark decelerator. The origin of the DC component in the OH signal is that the duration of the probe window is too short to remove all the molecules (regardless of the position of the window). The bottom panel in Fig. 2 shows the experimental data Fourier transformed to the frequency domain. The vertical dashed lines indicate breathing-mode trap frequencies determined from our full simulations of molecule dynamics in the potential calculated with finite element modeling for our actual decelerator geometry. The simulated frequencies agree well with the experimental ones.

Besides the simple comparison of the calculated and measured trap frequencies, we also measure other characteristics enabling a deeper understanding of the transverse dynamics in the Stark decelerator. We study how the amplitude (modulation depth) and phase of the oscillations depend on the applied voltage, $\Delta V$, and duration of the probe window, $T_{pro}$, see Figs. 3 and 4. The black points in Figs. 3 and 4 are experimental data. The actual experimental oscillatory signal is not perfectly periodic, and after a few oscillations can be considerably deformed, see the top panel in Fig. 2. Possible reasons of these imperfections are either slight mechanical deflection of the decelerator rods or inhomogeneous pin spacing. We reduce the influence of these effects by fitting a sine function to the first oscillation period only.

To understand the dynamics of the transverse motion and interpret the experimental data, we perform corresponding numerical Monte Carlo simulations, see red curves in Figs. 3 and 4. In the simplest case, we assume that after the supersonic expansion the spatial and velocity distributions are normal and have the same standard deviations in both transverse directions, i.e., $\sigma_x = \sigma_y$ and $\sigma_{v_x} = \sigma_{v_y}$. Molecules enter the decelerator after 38-cm-long free flight. The transverse motion of the molecules inside the decelerator was modeled with a harmonic effective trap whose frequency was taken from our full Monte Carlo simulations. The harmonic-effective-trap approximation is justified because, during the first oscillation period, the dispersion of the phase of the transverse motion due to anharmonicity is negligible. In this approach the only

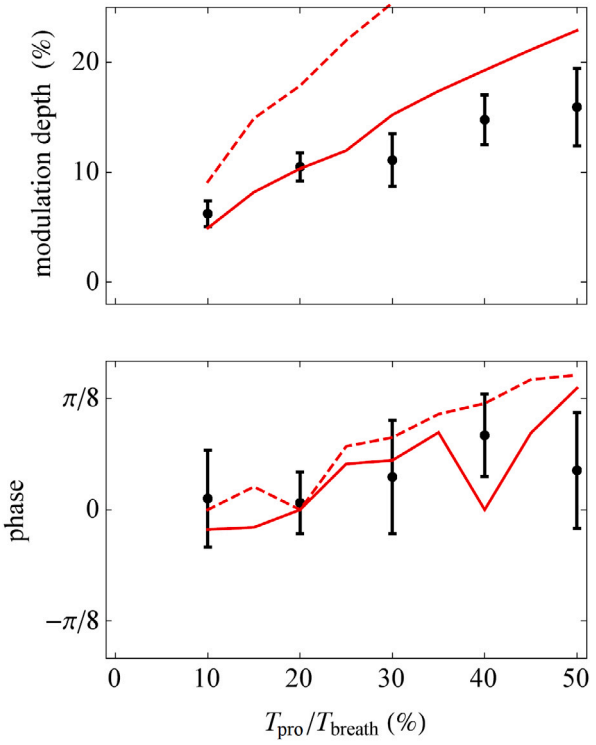


**Fig. 4.** Modulation depth and phase of the breathing mode of transverse-motion oscillations as a function of the probe window duration, $T_{pro}$, normalized to the breathing-mode period $T_{breath}$. The amplitude is normalized to the offset (the mean value) in the OH signal. The black points are experimental data and the red lines are results of our simulations. The dashed and solid lines are the results of simulations without and with molecules thermalization, respectively. Both the experiment and simulations were carried out for a decelerator voltage $\Delta V$ = 12 kV. The error bars are 1$\sigma$ standard uncertainties retrieved from the fits.

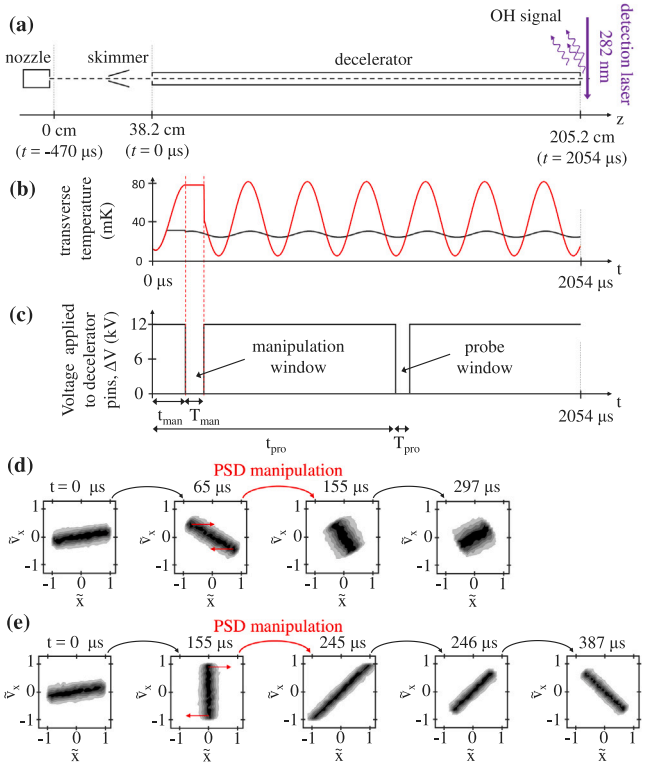


**Fig. 5.** Manipulation of the transverse oscillations inside a Stark decelerator. (a) Experimental setup. (b) Simulations of the transverse temperature of OH molecules for two different delays of the manipulation window ($t_{man}$). The black and red lines correspond to $t_{man}$ = 65 and 155 µs, respectively. (c) Voltage applied to decelerator pins. The DC voltage is interrupted for $T_{man}$ time to manipulate the phase-space distribution and for $T_{pro}$ to detect the resulting transverse oscillations. (d) and (e) Simulations of the phase-space dynamics for $t_{man}$ = 65 and 155 µs, respectively. In panel (e) we add one more intermediate state, $t$ = 246 µs, to show how the distribution looks when the molecules that do not fit the decelerator phase-space acceptance are removed from the plot. Note that between $t$ = 155 and 245 µs the electric field is off and some fraction of the molecules manage to escape the phase-space acceptance and are not retrapped when the field is on again. (For interpretation of the references to color in this figure legend, the reader is referred to the web version of this article.)

parameters of our simulations that need to be adjusted to experimental data are $\sigma_{x/y}$ and $\sigma_{v_{x/y}}$. However, within this simple picture, our simulations cannot reproduce the experimental observation from Figs. 3 and 4. The best adjustment for the voltage dependence is shown in Fig. 3 with the dashed red lines; the corresponding parameters are $\sigma_{x/y}$ = 3.0 mm and $\sigma_{v_{x/y}}$ = 9.9 m/s. For this initial distribution the probe-window-duration dependence gives even worse agreement with experimental data, see the dashed red lines in Fig. 4. One may consider different origins of this discrepancy among which the most likely ones seem to be thermalization and non-Gaussian initial distribution [29]. The experimental data accessible here does not allow us to uniquely resolve the origin of the discrepancy, but we tested one of them (the thermalization effect) showing that it allows us to reach a much better consistency between experiment and simulations with only one more adjustable parameter. We model the thermalization with a simple phenomenological approach in which a randomly chosen fraction of the molecules completely thermalizes while all the others remain unaffected. We model molecular thermalization at the decelerator entrance by randomly choosing a phase-space location within the decelerator's phase-space acceptance for a fraction $\beta$ of the total ensemble. For $\beta$ = 1 there is no thermalization and all the molecules undergo a free expansion from the valve to the decelerator entrance. In the opposite case of $\beta$ = 0, all the molecules are thermalized at the entrance of the decelerator. The solid red lines in Figs. 3 and 4 show the results of our Monte Carlo simulations that include this simple model of the thermalization effect. The corresponding values of the adjusted parameters are $\sigma_{x/y}$ = 2.0 mm, $\sigma_{v_{x/y}}$ = 28 m/s and $\beta$ = 0.4. The same parameters were assumed for the simulations from Figs. 1(b), (c) and (e). One remaining disagreement occurs at 2 kV voltage in the phase shift plot for Fig. 3. The success of the $\beta$ parameter otherwise suggests that collisions between molecules of interest and the decelerator geometry are certainly playing some role. If these collisions were to result not in a completely pure rethermalizing but a slight focus effect as well, this could give rise to the extra phase shift observed at lowest voltages. It should be noted that the $\beta$ parameter is a phenomenological parameter; it effectively compensates the contributions from different effects that occur on the way from the valve to the decelerator.

## 4. Manipulation of the transverse motion

We demonstrate that a similar approach of applying off-windows within the deceleration sequence can be used to manipulate the phase-space distribution and to observe the resulting transverse oscillations. In addition to the probe window we introduce a manipulation window. We consider two cases. In the first one, the phase-space distribution is stretched/squeezed along the transverse spatial dimensions during a short free-flight off-window, see Section 4.1. In the second approach, the phase-space distribution is rotated and stretched/squeezed at the same time, see Section 4.2.

### 4.1. Free-flight manipulation window

Our approach of manipulating the transverse phase-space in a Stark decelerator is shown in Fig. 5. Besides the probe window (which plays

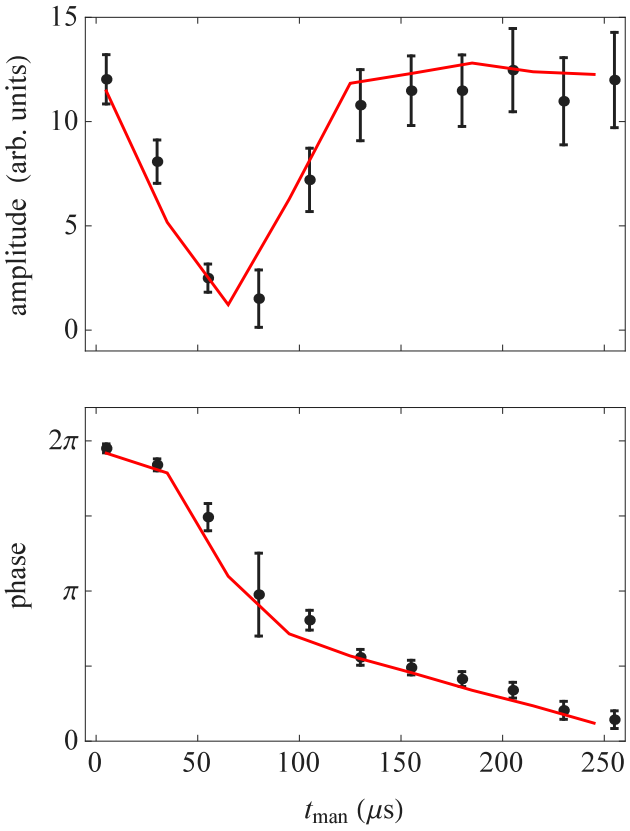


**Fig. 6.** Controlling the transverse motion with a free-flight manipulation window. The upper and lower plots show the amplitude and phase of the breathing-mode transverse oscillations as a function of the manipulation window delay ($t_{\mathrm{man}}$). The black points are experimental data and the red lines are results of our simulations. Both the experiment and simulations were carried out for the duration of the manipulation window $T_{\mathrm{man}} = 90$ μs. The error bars are $1\sigma$ standard uncertainties retrieved from the fits.

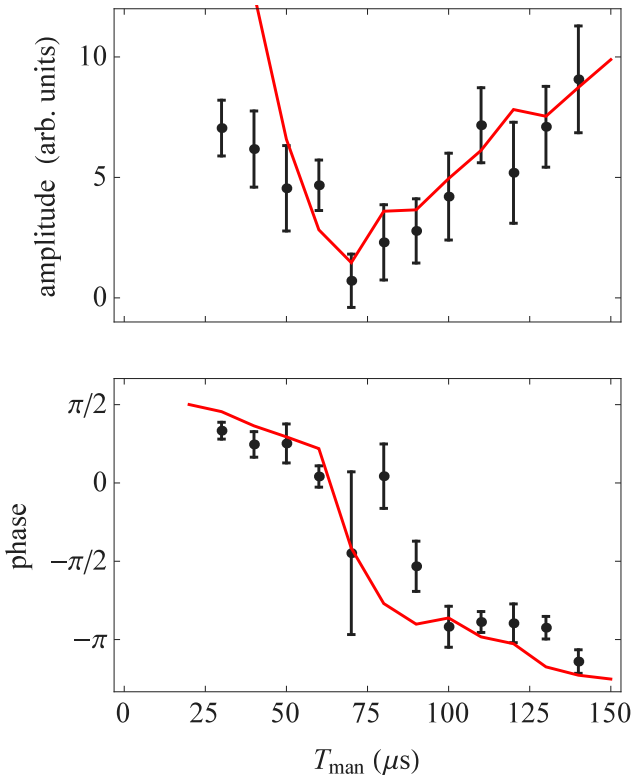


**Fig. 7.** Controlling transverse motion with a free-flight manipulation window. The upper and lower plots show the amplitude and phase of the breathing-mode transverse oscillations as a function of duration of the manipulation window, $T_{\mathrm{man}}$. The black points are experimental data and the red lines are simulation results. Both the experiment and simulations are carried out with the manipulation window delay $t_{\mathrm{man}} = 65$ μs. The error bars are $1\sigma$ standard uncertainties retrieved from the fits.

the same role as discussed in Section 3), we introduce another off-window that allows us to manipulate the phase space distribution, see Fig. 5(c). The simulations and experimental data presented in this section are for $\Delta V = 12$ kV. The effect of the manipulation window depends dramatically on the time position of the window, $t_{\mathrm{man}}$ (i.e., its relation to the phase of the phase-space oscillations). We investigate two cases. In the first case, the manipulation window starts when the anisotropy axis of the phase-space distribution is about 45° from reaching the vertical orientation, see the $t = t_{\mathrm{man}} = 65$ μs plot in Fig. 5(d). When the electric field is off, the molecular ensemble undergoes free flight during which the distribution is squeezed in the spatial $x$ (horizontal in our plots) direction. In Fig. 5, the duration of the manipulation window, $T_{\mathrm{man}}$, is 90 μs. As a result, the anisotropy of the phase-space distribution is considerably reduced and the amplitude of the corresponding oscillations of the transverse temperature is much smaller, see the black curve in Fig. 5(b). In the second case, the manipulation window starts when the anisotropy axis of the phase-space distribution reaches its vertical orientation, see the $t = t_{\mathrm{man}} = 155$ μs plot in Fig. 5(e). In this case, the ensemble free flight during the off-window results in stretching of the phase-space distribution in the spatial $x$ direction, see plot $t = 245$ μs in Fig. 5(e). After this stage some fraction of the molecules do not fit the decelerator phase-space acceptance anymore; compare plots $t = 245$ μs and 246 μs (in the first one all the molecules are present, while in the second one only those fitting the decelerator phase-space acceptance are kept). As a result we obtain a more anisotropic phase-space distribution than initially. The corresponding transverse temperature oscillations are shown as a red curve in the panel (b). Comparison of Figs. 5(d) and (e) shows that by tuning the time position of the manipulation window, $t_{\mathrm{man}}$, we can manipulate the transverse phase-space distribution from almost isotropic to strongly anisotropic.

We observe the resulting phase-space distribution in our experiment by applying the same detection method as discussed in Section 3. After the manipulation stage, we vary the location of a probe window and observe oscillations in the OH fluorescence signal detected after the decelerator. The amplitude of these oscillations reflects the anisotropy of the transverse phase-space distribution. In Fig. 6, we show the amplitude of the OH signal oscillations as a function of the manipulation window position, $t_{\mathrm{man}}$. The black points are the experimental data and red lines the simulations (using an effective harmonic trap approximation). The experimental data clearly confirm that we can use the manipulation window to control the transverse phase-space distribution. The minimum in the oscillation amplitude is anticorrelated with the total number of detected molecules; at the amplitude minimum the number of molecules is higher approximately by 20%. Additionally, a similar effect can be reached by tuning the manipulation window width, $T_{\mathrm{man}}$, see Fig. 7.

It should be noted that, in contrast to the simulations from Section 3 (Figs. 3 and 4), for phase-space manipulation experiments (Sections 4.1 and 4.2), we could not fully simulate a complete propagation from the supersonic valve all the way to the detection zone. The reason is that for studying only the detection scheme, Section 3, we measure only the first oscillation at the beginning of the decelerator. For the manipulation experiments we can only apply the probe window after a few oscillation periods when the influence of systematic perturbation (such as uneven pins spacing or decelerator bending) accumulates and the OH signal can be far from perfect, see the top panel in Fig. 2. Therefore in our

simulations for the phase-space manipulation experiments we do not propagate the initial phase-space distribution (determined in Section 3) all the way from valve to decelerator, but we adjust the phase-space distribution at the decelerator entrance such as to best reproduce the experimental data (this way we effectively compensate the influence of decelerator imperfections by adjusting the initial distribution). Despite this imperfection, our simulations give a clear and coherent explanation of the processes underlying the formation of the experimental features shown Figs. 6 and 7; note that the simulations of the evolution of the transverse phase-space distribution shown in Figs. 5(d) and (e) come from the same simulation runs as the red curves in Fig. 6.

The manipulation of the transverse motion demonstrated in this section involves the delta kick cooling (DKC) [24] in transverse dimensions. DKC is based on two steps. First, a well-localized ensemble of atoms or molecules undergoes a free flight. Then the phase-space distribution is rotated which results in narrowed distribution in the momentum direction. This is exactly what we obtained in a part of the experiment discussed in the previous section. We start from the well-localized ensemble of molecules, see the 155 μs panel in Fig. 5(e), which undergoes a free flight expansion along the spatial dimension (from $t = 155$ to 245 μs). Then the ensemble is rotated and reaches horizontal orientation at $t = 317$ μs (not shown in Fig. 5(e)) when the momentum distribution is narrowed. The two stages of the DKC are also seen in Fig. 5(b). The temperature is constant during the free flight period (the period between the two vertical dashed red lines). Then the transverse temperature drops as the phase-space distribution rotates (the DKC occurs during the first quarter of the sine oscillation after the second vertical dashed red line; the sudden drop of the temperature is caused by the fact that the hot fraction of the ensemble flew out from the trap during the free flight stage and is not related to DKC).

### 4.2. Enforced-rotation manipulation window

From the perspective of the phase-space evolution the manipulation off-window stretches or squeezes (depending on its phase relation to the phase-space oscillations) the distribution anisotropy in the spatial direction. Here we demonstrate a similar technique, but instead of letting the molecules undergo a free flight during the manipulation window, we enforce phase-space rotation along an arbitrarily defined ellipse.

Within the effective harmonic trap approximation, the maximum amplitudes in spatial, $x_0$, and velocity, $v_0$, dimensions are related by $v_0 = \omega x_0$. If we use $x_0$ and $v_0$ to normalize the spatial and velocity coordinates, $\tilde{x} = x/x_0$ and $\tilde{v}_x = v_x/v_0$ (as we did in Section 2), the trajectories are circular and the evolution in phase-space is simply a rotation of the distribution, see Fig. 1(c). If we suddenly switch the voltage applied across the decelerator pins then the trajectories will become elliptic. For higher voltages the major axis of ellipse will be oriented vertically, while for lower, horizontally. We explore this property to manipulate the transverse phase-space distribution. Similar to the previous section, we introduce the manipulation window, but instead of turning the voltage off we change its value. Then the manipulation window rotates the distribution along an arbitrarily chosen ellipse. Note that the manipulation off-window considered in the previous section is a special case of the present approach with the ellipse infinitely stretched in the horizontal direction.

We show the results of experimental implementation of this approach in Fig. 8; the black points are experimental data and red lines are simulations. In this case the DC voltage applied to decelerator was $\Delta V = 6$ kV, and during the manipulation window it was switched to 12 kV. Similarly to the manipulation off-window, also here the final transverse phase-space distribution depends on the time position of the manipulation window, $t_{\mathrm{man}}$, which we use as a parameter that allow us to control the amplitude of the transverse phase-space distribution. It should be noted that in the simulation shown in Fig. 8 we use exactly the same initial phase-space distribution as in Section 4.1 (Figs. 6 and 7).

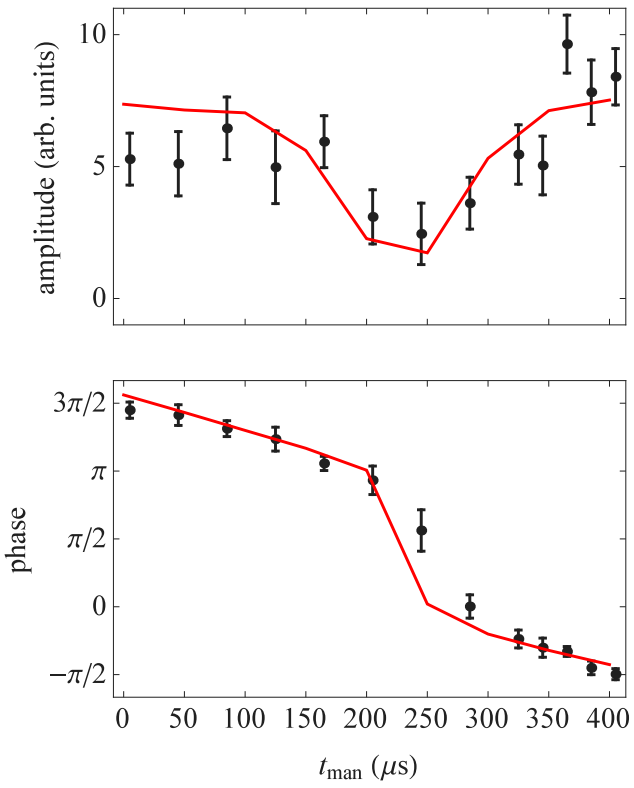


**Fig. 8.** Controlling the transverse motion with an enforced-rotation manipulation window. The upper and lower plots show the amplitude and phase of the breathing-mode transverse oscillations as a function of the manipulation window delay ($t_{\mathrm{man}}$). The black points are experimental data and the red lines are results of our simulations. Both the experiment and simulations are carried out with duration of the manipulation window $T_{\mathrm{man}} = 142$ μs. The error bars are $1\sigma$ standard uncertainties retrieved from the fits.

## 5. Discussion and conclusions

In this paper, we showed an experimental technique enabling measurement and manipulation of the transverse phase-space distribution in a Stark decelerator. We introduced a probe window that allowed us to track the transverse motion in a Stark decelerator along its entire length. A good agreement was reached between our Monte Carlo simulations of the evolution of the transverse phase space and the corresponding experimental data after incorporating a simple model of molecule thermalization at the decelerator entrance. The measured frequency of the transverse oscillations was consistent with our simulations based on the decelerator geometry and electric field distribution. We introduced a second off-window that allowed us to manipulate the transverse phase-space distribution. During the manipulation off-window the molecules undergo a free expansion, and depending on the time delay of the manipulation window, we could tune the phase-space distribution anisotropy in a well controlled way. For a specific choice of the parameters of the manipulation sequence, we obtained the delta kick cooling in the transverse directions. We also tested a modified version of the manipulation window in which we did not turn off the decelerator electric field but changed its magnitude, which allowed us to manipulate the transverse motion by rotating the phase-space distribution along an arbitrarily chosen ellipse. The ability to adjust the transverse phase-space distribution can be helpful for efficient loading of molecular traps placed at the output of the decelerator or to have better control over molecular collision conditions in beam experiments.

## CRediT authorship contribution statement

**Piotr Wcisło:** Conceptualization, Investigation, Writing – original draft, Writing – review & editing. **Hao Wu:** Conceptualization, Investigation, Writing – original draft, Writing – review & editing. **David Reens:** Conceptualization, Investigation, Writing – original draft, Writing – review & editing. **Alexander Aeppli:** Conceptualization, Investigation, Writing – original draft, Writing – review & editing. **Jun Ye:** Conceptualization, Investigation, Writing – original draft, Writing – review & editing.

## Declaration of competing interest

The authors declare that they have no known competing financial interests or personal relationships that could have appeared to influence the work reported in this paper.

## Acknowledgments

Funding for this work is provided by NSF-1734006, ARO MURI, and NIST. P.W. acknowledges support from the Polish Ministry of Science and Higher Education "Mobility Plus" Program and the National Science Centre, Poland, Project No. 2019/35/B/ST2/01118.

## References

[1] H. Kallmann, F. Reiche, Z. Phys. 6 (1921) 352.
[2] S.Y.T. van de Meerakker, H.L. Bethlem, N. Vanhaecke, G. Meijer, Chem. Rev. 112 (2012) 4828, http://dx.doi.org/10.1021/cr200349r.
[3] H.L. Bethlem, G. Berden, G. Meijer, Phys. Rev. Lett. 83 (1999) 1558, http://dx.doi.org/10.1103/PhysRevLett.83.1558.
[4] H.L. Bethlem, F.M.H. Crompvoets, R.T. Jongma, S.Y.T. van de Meerakker, G. Meijer, Phys. Rev. A 65 (2002) 053416, http://dx.doi.org/10.1103/PhysRevA.65.053416.
[5] J.R. Bochinski, E.R. Hudson, H.J. Lewandowski, G. Meijer, J. Ye, Phys. Rev. Lett. 91 (2003) 243001, http://dx.doi.org/10.1103/PhysRevLett.91.243001.
[6] M.R. Tarbutt, H.L. Bethlem, J.J. Hudson, V.L. Ryabov, V.A. Ryzhov, B.E. Sauer, G. Meijer, E.A. Hinds, Phys. Rev. Lett. 92 (2004) 173002, http://dx.doi.org/10.1103/PhysRevLett.92.173002.
[7] S. Jung, E. Tiemann, C. Lisdat, Phys. Rev. A 74 (2006) 040701, http://dx.doi.org/10.1103/PhysRevA.74.040701.
[8] J.J. Gilijamse, S. Hoekstra, N. Vanhaecke, S. van de Meerakker, G. Meijer, Eur. Phys. J. D 57 (2010) 33, http://dx.doi.org/10.1140/epjd/e2010-00008-9.
[9] B.C. Sawyer, B.K. Stuhl, D. Wang, M. Yeo, J. Ye, Phys. Rev. Lett. 101 (2008a) 203203, http://dx.doi.org/10.1103/PhysRevLett.101.203203.
[10] B.C. Sawyer, B.L. Lev, E.R. Hudson, B.K. Stuhl, M. Lara, J.L. Bohn, J. Ye, Phys. Rev. Lett. 98 (2007) 253002, http://dx.doi.org/10.1103/PhysRevLett.98.253002.
[11] D. Reens, H. Wu, T. Langen, J. Ye, Phys. Rev. A 96 (2017) 063420, http://dx.doi.org/10.1103/PhysRevA.96.063420.
[12] S.N. Vogels, J. Onvlee, S. Chefdeville, A. van der Avoird, G.C. Groenenboom, S.Y.T. van de Meerakker, Science 350 (2015) 787, http://dx.doi.org/10.1126/science.aad2356.
[13] S.N. Vogels, T. Karman, J. Kłos, M. Besemer, J. Onvlee, A. van der Avoird, G.C. Groenenboom, S.Y.T. van de Meerakker, Nature Chem. 10 (2018) 435, http://dx.doi.org/10.1038/s41557-018-0001-3.
[14] E.R. Hudson, H.J. Lewandowski, B.C. Sawyer, J. Ye, Phys. Rev. Lett. 96 (2006) 143004, http://dx.doi.org/10.1103/PhysRevLett.96.143004.
[15] C. Cheng, A.P.P. van der Poel, P. Jansen, M. Quintero-Pérez, T.E. Wall, W. Ubachs, H.L. Bethlem, Phys. Rev. Lett. 117 (2016) 253201, http://dx.doi.org/10.1103/PhysRevLett.117.253201.
[16] A.P.P. van der Poel, P.C. Zieger, S.Y.T. van de Meerakker, J. Loreau, A. van der Avoird, H.L. Bethlem, Phys. Rev. Lett. 120 (2018) 033402, http://dx.doi.org/10.1103/PhysRevLett.120.033402.
[17] J.R. Bochinski, E.R. Hudson, H.J. Lewandowski, J. Ye, Phys. Rev. A 70 (2004) 043410, http://dx.doi.org/10.1103/PhysRevA.70.043410.
[18] Y. Shyur, J.A. Bossert, H.J. Lewandowski, J. Phys. B: At. Mol. Opt. Phys. 51 (2018) 165101, http://dx.doi.org/10.1088/1361-6455/aad1b0.
[19] S.Y.T. van de Meerakker, N. Vanhaecke, H.L. Bethlem, G. Meijer, Phys. Rev. A 73 (2006) 023401, http://dx.doi.org/10.1103/PhysRevA.73.023401.
[20] S.Y.T. van de Meerakker, H.L. Bethlem, G. Meijer, Nature Phys. 4 (2008) 595, http://dx.doi.org/10.1038/nphys1031.
[21] B.C. Sawyer, B.K. Stuhl, B.L. Lev, J. Ye, E.R. Hudson, Eur. Phys. J. D 48 (2008b) 197, http://dx.doi.org/10.1140/epjd/e2008-00097-y.
[22] L. Scharfenberg, H. Haak, G. Meijer, S.Y.T. van de Meerakker, Phys. Rev. A 79 (2009) 023410, http://dx.doi.org/10.1103/PhysRevA.79.023410.
[23] D. Reens, H. Wu, A. Aeppli, A. McAuliffe, P. Wcisło, T. Langen, J. Ye, Phys. Rev. Res. 2 (2020) 033095, http://dx.doi.org/10.1103/PhysRevResearch.2.033095.
[24] H. Ammann, N. Christensen, Phys. Rev. Lett. 78 (1997) 2088, http://dx.doi.org/10.1103/PhysRevLett.78.2088.
[25] H. Wu, D. Reens, T. Langen, Y. Shagam, D. Fontecha, J. Ye, Phys. Chem. Chem. Phys. 20 (2018) 11615, http://dx.doi.org/10.1039/C8CP00962G.
[26] U. Even, Adv. Chem. 2014 (2014) 636042, http://dx.doi.org/10.1155/2014/636042.
[27] H. Wu, (Ph.D. dissertation), 2019.
[28] D. Reens, (Ph.D. dissertation), 2019.
[29] H.C.W. Beijerinck, N.F. Verster, Physica B+C 111 (1981) 327, http://dx.doi.org/10.1016/0378-4363(81)90112-1.